

# A TRAJECTORY-SPECIFIC APPROACH FOR CALCULATING THE REQUIRED HOLDING FORCE FOR SURFACE GRIPPERS

Tobias Eberhardt<sup>1,2,4,\*</sup>, Valentin Stegmaier<sup>1,3,4</sup>, Walter Schaaf<sup>4</sup>, Alexander Verl<sup>2</sup>

<sup>1</sup> Graduate School of Excellence advanced Manufacturing Engineering (GSaME), University of Stuttgart, Nobelstraße 12, 70569 Stuttgart, Germany

<sup>2</sup> Institute for Control Engineering of Machine Tools and Manufacturing Units, University of Stuttgart, Seidenstraße 36, 70174 Stuttgart, Germany

<sup>3</sup> Institute of Industrial Automation and Software Engineering, University of Stuttgart, Pfaffenwaldring 47, 70569 Stuttgart, Germany

<sup>4</sup> J. Schmalz GmbH, Pre-Development, Johannes-Schmalz-Str. 1, 72293 Glatten, Germany

\* Corresponding author: Tel.: +49 7443 2403-7516; E-mail address: tobias.eberhardt@gsame.uni-stuttgart.de

---

## ABSTRACT

With increasing demands on the productivity and efficiency of manufacturing plants and rising energy costs, manufacturers of components and systems in industrial automation must also ensure that their products are used to their full potential in the intended application. This applies to automated handling with vacuum handling systems too. The energy consumption of such systems is highly dependent on the required holding force. In industrial automation, the required holding force is calculated from a few discrete positions of the surface gripper and the gripping object from the handling process. These positions are called load cases. However, the continuous transition between the kinematic positions of the individual load cases is not observed. The new approach presented in this paper allows an accurate calculation of the holding force required in the transition position when moving along a trajectory. Based on this new approach, the energy consumption of the vacuum handling system can be reduced. A validation with several experiments show good results.

**Keywords:** Holding force, Surface gripper, Energy efficiency, Vacuum handling system

---

## 1. INTRODUCTION

Handling systems are common and important subsystems of modern production plants. A handling system is used to load and unload workpieces to and from various stations in the production plant. They are also used to transport workpieces between processing stations. Vacuum handling systems are often used for such handling tasks [1]. One of their main advantages is the ability to grip objects from only one side using surface grippers in form of suction cups. This allows vacuum handling systems to be easily adapted to different shapes, weights and sizes of objects without the need of modifying the system. These features make vacuum handling systems an attractive solution for future flexible production systems [2].

In general, a vacuum handling system consists of components from six groups, which are vacuum generators, connections, fasteners, switching and system monitoring elements, valves, and suction cups [3]. The three most crucial components in the design of a vacuum handling system are vacuum generators, connections and suction cups [4]. For the purposes of the following considerations, the suction cup will be used as a representative of surface grippers.

The holding force that can be achieved by a vacuum handling system with respect to a gripping object depends largely on the effective suction area and the pressure difference achieved in the suction cup with respect to the environment. The effective suction area is mainly determined by the number of cups used, their size and type, and is therefore highly dependent on the geometric dimensions of the

gripping object. The pressure difference that can be achieved in a leakage-free system depends on the vacuum generator used, the evacuation time and the internal flow resistance of the system and is often referred to as the vacuum level. The vacuum level correlates directly with the energy consumption of the system, with particularly high vacuum levels being very energy intensive [5], [6]. **Figure 1** shows a typical structure of a simple vacuum handling system and an industrial application.



**Figure 1:** Typical structure of a vacuum handling system and a typical industrial application [7]

In practice, the holding force required for handling is usually calculated using discrete load cases. However, there are many applications in industry, such as rotating the gripping object with a robot, which cannot be adequately represented using these discrete load cases. See **Figure 2**. To compensate for this uncertainty, a high safety factor is added to the calculated holding force [2].

The new approach outlined below aims to change this. For this purpose, the state of the art is presented in section 2. In section 3, the mathematical formulation of the new approach is described. This is followed by experiments for validation in section 4. This section also compares the calculated and measured results. The paper ends with a short conclusion and an outlook.

## 2. STATE OF THE ART

After describing the calculation of the vacuum holding force of a vacuum handling system, existing approaches to calculate the theoretical holding force are presented.

### 2.1. Calculation of the suction force

According to Hesse [8], the holding force that can be applied by a vacuum suction cup depends on the effective suction area  $A$ , the pressure difference  $\Delta p$ , the safety factor  $S$ , the deformation coefficient  $n_3$  to take into account the suction lip deformation due to the pressure drop and the efficiency  $\eta$  (leakage losses of the system). It can be calculated as follows:

$$F_{Suction} = \Delta p \cdot A \cdot \eta \cdot n_3 \cdot \frac{1}{S} = (p_0 - p_U) \cdot A \cdot \eta \cdot n_3 \cdot \frac{1}{S} \quad (1)$$

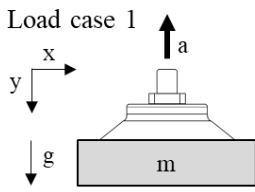
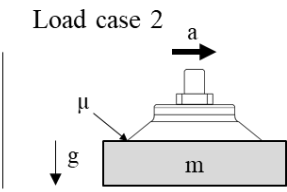
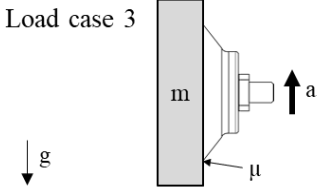
The holding force  $F_{Suction}$  exerted by the suction cup must be greater than the theoretical holding force  $F_{Th}$  required by the process and the gripping object for safe handling.

$$F_{Suction} \geq F_{Th} \quad (2)$$

### 2.2. Existing approaches to calculate the required holding force

An existing approach is to define and mathematically describe some basic load cases in order to calculate the theoretically required holding force [9], [1], [2], [10]. For this purpose, the suction cup and the gripping object are considered either in horizontal alignment or in vertical alignment. **Figure 2** shows the described alignments of the suction cup and the gripping object. For the horizontal

alignment of the suction cup and the gripping object, a further distinction is often made between a vertical and a horizontal movement [9]. This subdivision is often referred to as load cases 1 to 3. Load case 1 is considered the most favourable and load case 3 the least favourable [9].

horizontal alignment		vertical alignment
		
<p>Load case 1: <math>F_{Th} = m \cdot (g + a)</math> (3)</p>		<p>Load case 3: <math>F_{Th} = m \cdot \frac{(g + a)}{\mu}</math> (4)</p>
<p>Load case 2: <math>F_{Th} = m \cdot \left(g + \frac{a}{\mu}\right)</math> (5)</p>		

**Figure 2:** Load case 1 to 3 for handling systems

Hesse [8], on the other hand, combines load cases 1 and 2 described in **Figure 2** by splitting a force acting obliquely on the centre of mass into an  $x$  and  $y$  component based on the angle of attack. The individual components are then calculated according to load cases 1 and 2. The results are added together to give the theoretical holding force required. In addition, Hesse extends the load cases 1 and 2 just described by the case of off-centre force application in the case of an eccentric centre of mass of the gripping object in the gripping plane.

Spivak's [11] approach considers an inclined suction cup. However, Spivak focuses on the holding force applied by the suction cup at a given vacuum and vertical movement.

### 2.3. Conclusions from the introduction and the initial situation

The presented approaches describe only discrete alignments (horizontal/vertical) of the suction cup - gripping object combination and map them to up to three load cases. A trajectory specific calculation is therefore not possible. Furthermore, they neglect the tipping moment due to a spatial expansion of the gripping object. In addition, the holding force applied by the suction cup at a certain vacuum is dealt with. However, not with the theoretically necessary holding force.

## 3. NEW APPROACHES FOR CALCULATING THE REQUIRED TRAJECTORY SPECIFIC HOLDING FORCE

Two approaches are presented for calculating the required holding force. The first approach neglects the spatial expansion of the gripping object. This extension is included in the second approach. We assume a point mass. Its distance cannot be neglected. The influence of air resistance on the gripping object during handling is neglected in both approaches. The occurring forces and accelerations are divided into  $x$  and  $y$  or  $N$  and  $K$  components according to the coordinate systems used and are marked with an appropriate subscript. The accelerations in the  $x$  and  $y$  directions and the angle of rotation  $\alpha$  can be expressed as a function of time  $t$  to describe the trajectory of the combination of suction cups and gripping object. Accordingly, the theoretical holding force required  $F_{Th}$  is also time-dependent.

### 3.1. Approach 1: Theoretically necessary holding force without tipping moment

In this approach, the spatial expansion of the gripping object is neglected and instead the gripping object is assumed to be a point mass. The centre of gravity of the gripping object is at the centre of the support surface of the suction cup. **Figure 3** shows the mechanical modelling assumed for the mathematical formulation.

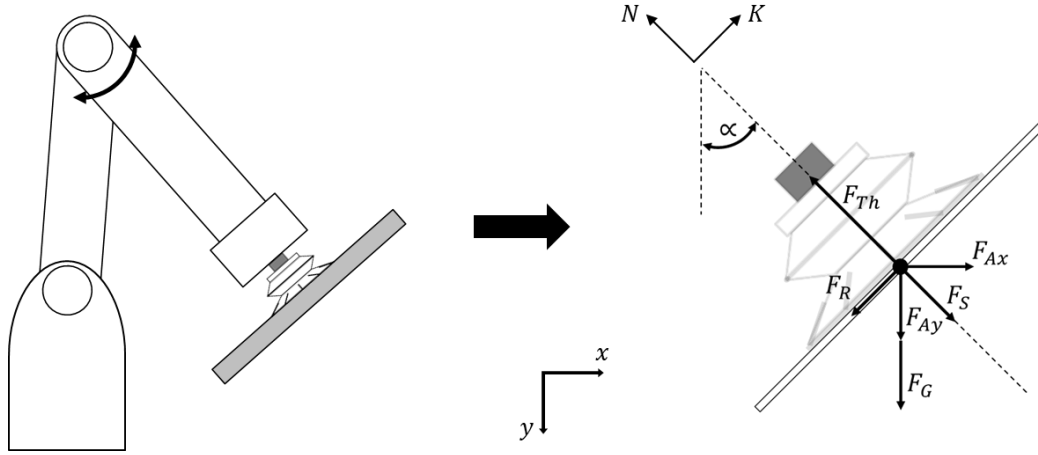


**Figure 3:** Mechanical modeling for thin gripping objects

To calculate the theoretically required holding force, static equilibrium with respect to the point mass is assumed. To do this, a second coordinate system is used with its principal axis in the direction of  $F_{Th}$ . The static equilibrium of inertia force  $F_A$  as a result of acceleration, weight force  $F_G$ , the suction restoring force  $F_S$  and the holding force  $F_{Th}$  along the  $N$ -axis then results as follows:

$$\sum F_i = 0 = F_{AxN} + F_{AyN} + F_{GN} + F_S - F_{Th} = 0 \quad (6)$$

The forces are transformed into the  $N$ - $K$  coordinate system according to the angle of rotation  $\alpha$ . The inertial forces can be transformed as follows:

$$F_{AxN} = F_{Ax} \cdot \sin(\alpha) = m \cdot a_x \cdot \sin(\alpha) \quad (7)$$

$$F_{AyN} = F_{Ay} \cdot \cos(\alpha) = m \cdot a_y \cdot \cos(\alpha) \quad (8)$$

$$F_{GN} = F_G \cdot \cos(\alpha) = m \cdot g \cdot \cos(\alpha) \quad (9)$$

The restoring force  $F_S$  of the suction cup is formulated as a function of the frictional force  $F_R$ . It depends on the magnitude of the frictional force and not on its direction. In the static case, it can be described by an equilibrium of the individual force components in the direction of the  $K$  axis. Converting the state of equilibrium to  $F_S$  gives the restoring force as follows:

$$F_S = \frac{|F_R|}{\mu} = \frac{|F_{Ax} \cdot \cos(\alpha) - (F_{Ay} + F_G) \cdot \sin(\alpha)|}{\mu} = m \cdot \frac{|a_x \cdot \cos(\alpha) - (a_y + g) \cdot \sin(\alpha)|}{\mu} \quad (10)$$

Substituting (7), (8), (9) and (10) into equation (6) gives the following formula for calculating the theoretical holding force  $F_{Th}$ :

$$F_{Th} = F_{Ax} \cdot \sin(\alpha) + (F_{Ay} + F_G) \cdot \cos(\alpha) + \frac{|F_{Ax} \cdot \cos(\alpha) - (F_{Ay} + F_G) \cdot \sin(\alpha)|}{\mu} \quad (11)$$

$$F_{Th} = m \cdot a_x \cdot \sin(\alpha) + m \cdot (a_y + g) \cdot \cos(\alpha) + m \cdot \frac{|a_x \cdot \cos(\alpha) - (a_y + g) \cdot \sin(\alpha)|}{\mu} \quad (12)$$

For an angle of rotation with  $\alpha$  of  $0^\circ$ , the combination of load cases 1 and 2 results from the state of the art. For an angle of rotation of  $\alpha = 90^\circ$ , load case 3 results from the state of the art. **Figure 4** shows the theoretical holding force required along the trajectory for a smooth  $90^\circ$  tilt of the robot from the horizontal position.

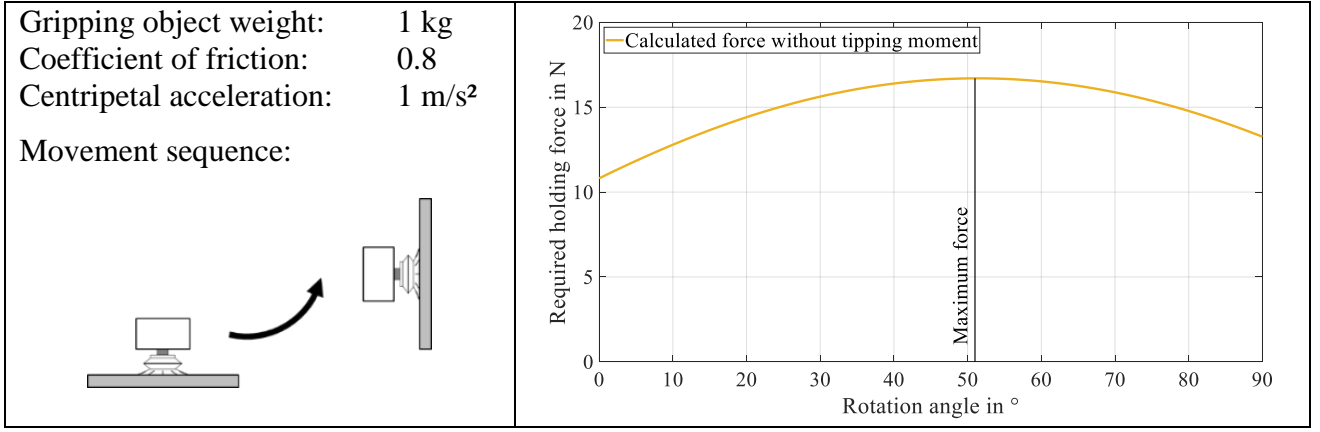


**Figure 4:** Theoretical required holding force when swivelling thin gripping objects

### 3.2. Approach 2: Theoretically necessary holding force with tipping moment

In the second approach, the gripping object has a spatial extension. However, the calculation still assumes that the centre of mass of the gripping object is on the same axis as the theoretically required holding force and that there is no relative displacement of the centre of mass during handling. **Figure 5** shows the corresponding modelling.

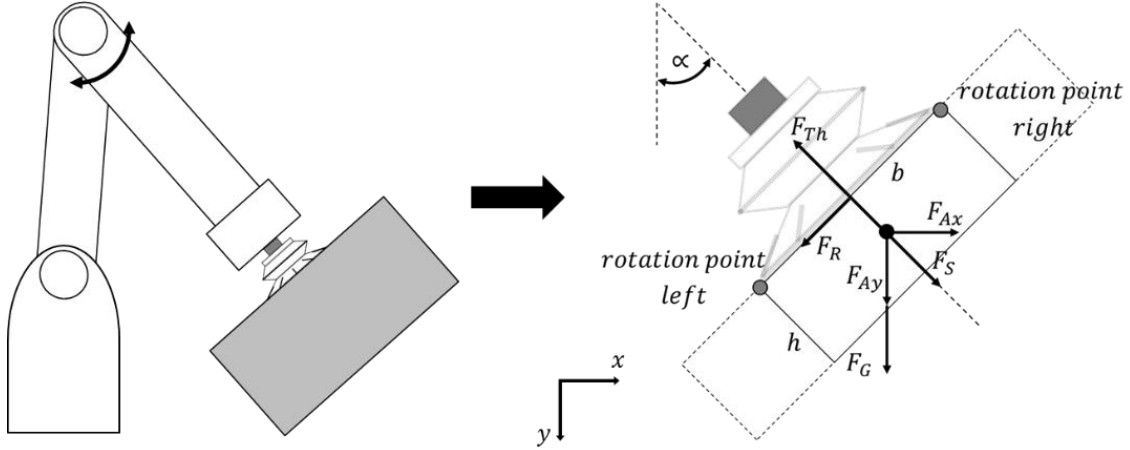


**Figure 5:** Mechanical modeling for gripping objects with spatial extension (h and b)

To calculate the required holding force, a static moment equilibrium is established around the left or right rotation point. The rotation point depends on the current angle of rotation  $\alpha$  and the ratio of the accelerations in the  $x$  and  $y$  directions, as well as the geometric dimensions of the gripping object, and is located either at the top or bottom edge of the suction cup. For reasons of clarity, the basic equations for the forces are not used in the following. The following equation for the static moment equilibrium results for the left rotation point:

$$\sum M_i = 0 = M_{Th} \pm M_{Ax} - M_G - M_S - M_{Ay} = 0 \quad (13)$$

For the right pivot point, the moment equilibrium is as follows:

$$\sum M_i = 0 = M_{Th} - M_{Ax} - M_G - M_S \pm M_{Ay} = 0 \quad (14)$$

$M_{Ax}$  at the left rotation point and  $M_{Ay}$  at the right rotation point have different effects on the moment equilibrium depending on the current rotation point. This must be taken into account in the geometric modelling of each moment. The modelling of the lever arms for both rotation points is shown in **Figure 6**.

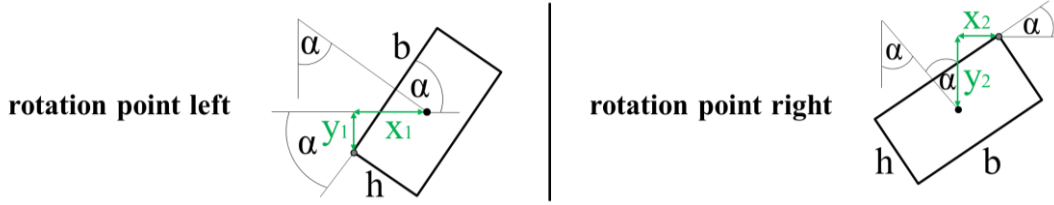


**Figure 6:** Left and right pivot points for moment equilibrium

According to **Figure 6**, the lever arms for the left rotation point can be described as follows:

$$x_1 = \frac{h}{2 \cdot \sin(\alpha)} + \cos(\alpha) \cdot \left( \frac{b}{2} - \frac{h}{2 \cdot \tan(\alpha)} \right) \quad (15)$$

$$y_1 = \frac{1}{2} \cdot (b \cdot \sin(\alpha) - h \cdot \cos(\alpha)) \quad (16)$$

The lever arms of the forces with respect to the right rotation point, on the other hand, result from **Figure 6** as follows:

$$x_2 = \frac{\cos(\alpha)}{2} \cdot (b - h \cdot \tan(\alpha)) \quad (17)$$

$$y_2 = \frac{h}{2 \cdot \cos(\alpha)} + \frac{\sin(\alpha)}{2} \cdot (b - h \cdot \tan(\alpha)) \quad (18)$$

Based on the geometric boundary conditions above, the following equations result for the moments of acceleration ( $M_{Ax}$  and  $M_{Ay}$ ), gravity ( $M_G$ ) and restoring ( $M_S$ ) for the left rotation point:

$$M_{Ax} = F_{Ax} \cdot \frac{1}{2} \cdot (b \cdot \sin(\alpha) - h \cdot \cos(\alpha)) \quad (19)$$

$$M_{Ay} = F_{Ay} \cdot \left( \frac{h}{2 \cdot \sin(\alpha)} + \cos(\alpha) \cdot \left( \frac{b}{2} - \frac{h}{2 \cdot \tan(\alpha)} \right) \right) \quad (20)$$

$$M_G = F_G \cdot \left( \frac{h}{2 \cdot \sin(\alpha)} + \cos(\alpha) \cdot \left( \frac{b}{2} - \frac{h}{2 \cdot \tan(\alpha)} \right) \right) \quad (21)$$

$$M_S = F_S \cdot \frac{b}{2} = \frac{|F_R|}{\mu} \cdot \frac{b}{2} = \frac{|F_{Ax} \cdot \cos(\alpha) - (F_{Ay} + F_G) \cdot \sin(\alpha)|}{\mu} \cdot \frac{b}{2} \quad (22)$$

Merging the equations (19), (20), (21), and (22) into (13) gives the following equation for the theoretically required holding force  $F_{Th}$  in relation to the left rotation point:

$$F_{Th} = \frac{F_{Ax}}{b} \cdot (b \cdot \sin(\alpha) - h \cdot \cos(\alpha)) + \frac{(F_{Ay} + F_G)}{b} \cdot \left( \frac{h}{\sin(\alpha)} + \cos(\alpha) \cdot \left( b - \frac{h}{\tan(\alpha)} \right) \right) + \frac{|F_{Ax} \cdot \cos(\alpha) - (F_{Ay} + F_G) \cdot \sin(\alpha)|}{\mu} \quad (23)$$

For the right pivot, the equations for the accelerations ( $M_{Ax}$  and  $M_{Ay}$ ), gravity ( $M_G$ ) and restoring ( $M_S$ ) are as follows:

$$M_{Ax} = F_{Ax} \cdot \left( \frac{h}{2 \cdot \cos(\alpha)} + \frac{\sin(\alpha)}{2} \cdot (b - h \cdot \tan(\alpha)) \right) \quad (24)$$

$$M_{Ay} = F_{Ay} \cdot \left( \frac{\cos(\alpha)}{2} \cdot (b - h \cdot \tan(\alpha)) \right) \quad (25)$$

$$M_G = F_G \cdot \left( \frac{\cos(\alpha)}{2} \cdot (b - h \cdot \tan(\alpha)) \right) \quad (26)$$

$$M_S = F_S \cdot \frac{b}{2} = \frac{|F_R|}{\mu} \cdot \frac{b}{2} = \frac{|F_{Ax} \cdot \cos(\alpha) - (F_{Ay} + F_G) \cdot \sin(\alpha)|}{\mu} \cdot \frac{b}{2} \quad (27)$$

Merging the equations (24), (25), (26), and (27) into (14) gives the following equation for the theoretically required holding force  $F_{Th}$  in relation to the right rotation point:

$$F_{Th} = \frac{F_{Ax}}{b} \cdot \left( \frac{h}{\cos(\alpha)} + \sin(\alpha) \cdot (b - h \cdot \tan(\alpha)) \right) + \frac{(F_{Ay} + F_G)}{b} \cdot (\cos(\alpha) \cdot (b - h \cdot \tan(\alpha))) + \frac{|F_{Ax} \cdot \cos(\alpha) - (F_{Ay} + F_G) \cdot \sin(\alpha)|}{\mu} \quad (28)$$

**Figure 7** shows an extension of the calculation of the theoretically required holding force for the swivel operation from **Figure 4** by a spatial extension of the gripping object.

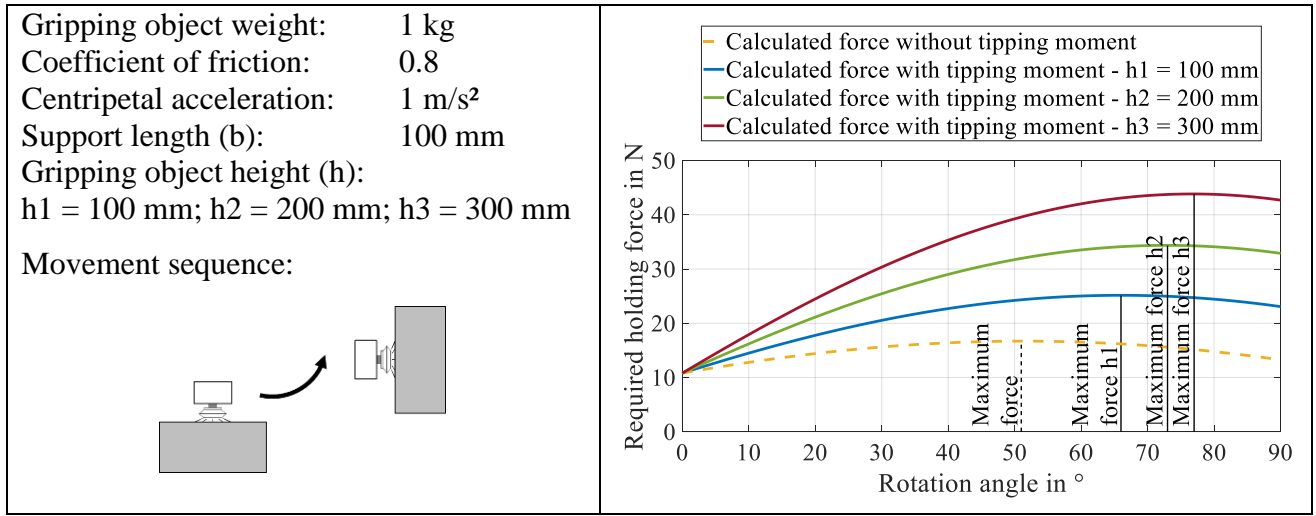


**Figure 7:** Theoretically required holding force when swivelling gripping objects with relevant thickness

### 3.3. Summary of the new approaches

The two approaches presented in sections 3.1 and 3.2 can be used to calculate the required holding force of the suction cup along any trajectory in the plane. **Figure 4** and **Figure 7** both show that the required force  $F_{Th}$  does not always have its maximum in one of the discrete load cases 1 to 3 according to the state of the art shown in **Figure 2**. Furthermore, the position of the maximum force is strongly dependent on the friction value and the ratio of the accelerations. Apart from that, the position of the centre of mass as a result of the spatial expansion of the gripping object also has a significant influence on the position of the maximum force as well as its magnitude. For this reason, designing using discrete load cases based on the worst-case scenario carries the risk of overestimating the maximum holding force. In addition to the swivel process itself, an intelligent choice of gripping object orientation can reduce the theoretical holding forces required for horizontal movement, for example. This allows a lower vacuum level and therefore lower energy absorption. **Figure 8** shows how, for an example application, a 6° adjustment results in a 17.7 % reduction in the holding force required.

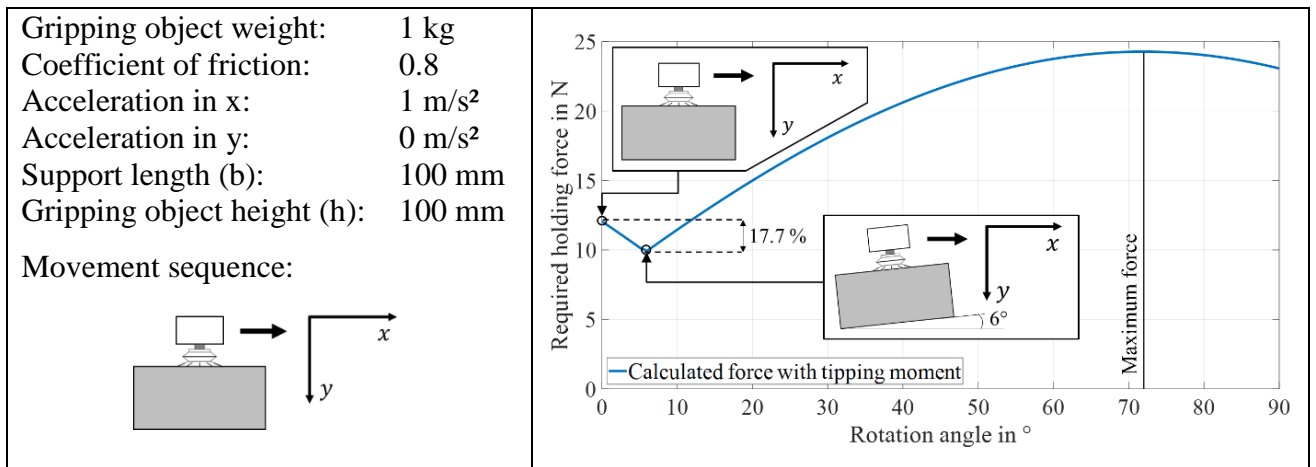


**Figure 8:** Reduce required holding force through clever alignment of the gripping object

## 4. VALIDATION

Several tests were carried out to validate the two new calculation methods described in section 3. For the calculation without overturning moment, a sheet metal of supposedly negligible thickness was chosen. On the other hand, for the calculation with tilting moment, a composite of two steel blocks was chosen. **Figure 9** shows the two parts and their main characteristics.

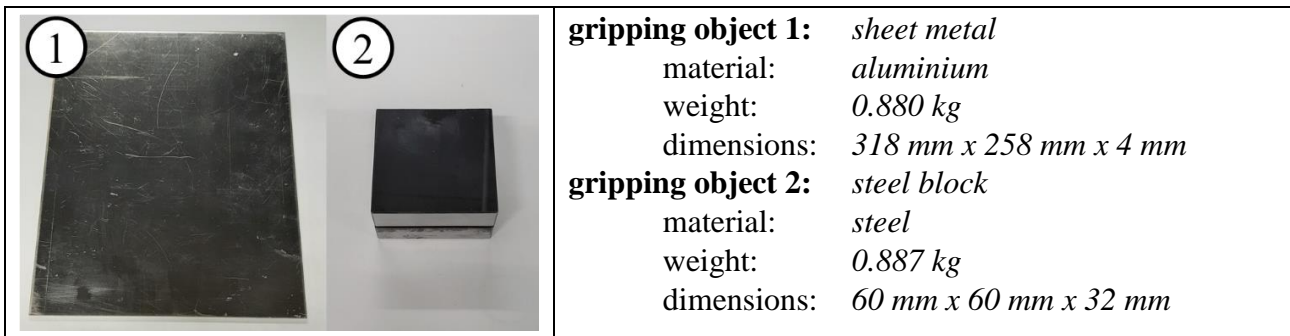


**Figure 9:** Test gripping objects used and their characteristics

For the suction cup, a seamless 3D printed sealing ring made of resin-acrylic-50 was chosen. This is inserted into a printed holder depending on the specific experimental setup. The combination of sealing ring and holder then forms the suction cup. The sealing rings and suction cups used in the respective test set-ups can be seen in **Figure 10**.

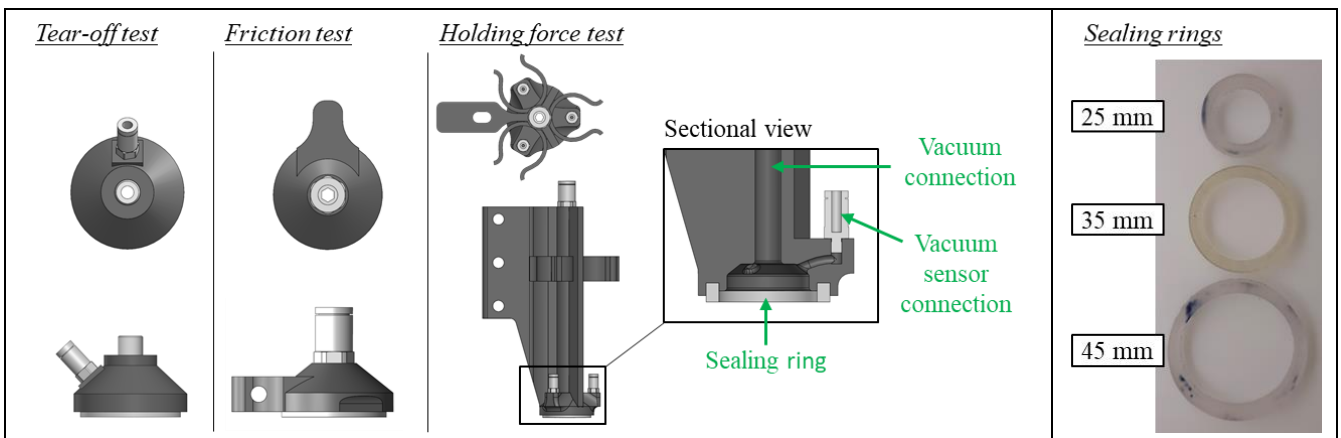


**Figure 10:** Suction cups and sealing rings used in the test set-ups

### 4.1. Determination of the suction cup diameter

In a first test, several tear-off tests were carried out to confirm the actual diameter  $d$  of the sealing ring. To do this, the seal was placed in another holder and pulled vertically off the test piece using a tensile testing machine. This was repeated at least three times for different vacuum levels. The vacuum was generated by an ejector (= vacuum generator) and manually adjusted to the appropriate level using a ball valve and a vacuum sensor. For evaluation, the maximum force in the force-displacement curve was determined representing the last point before, the cup lifts and is vented. At this point the handling system fails. The test set-up described and the test results obtained are shown in **Figure 11**. A 35 mm sealing ring was used for the tests.



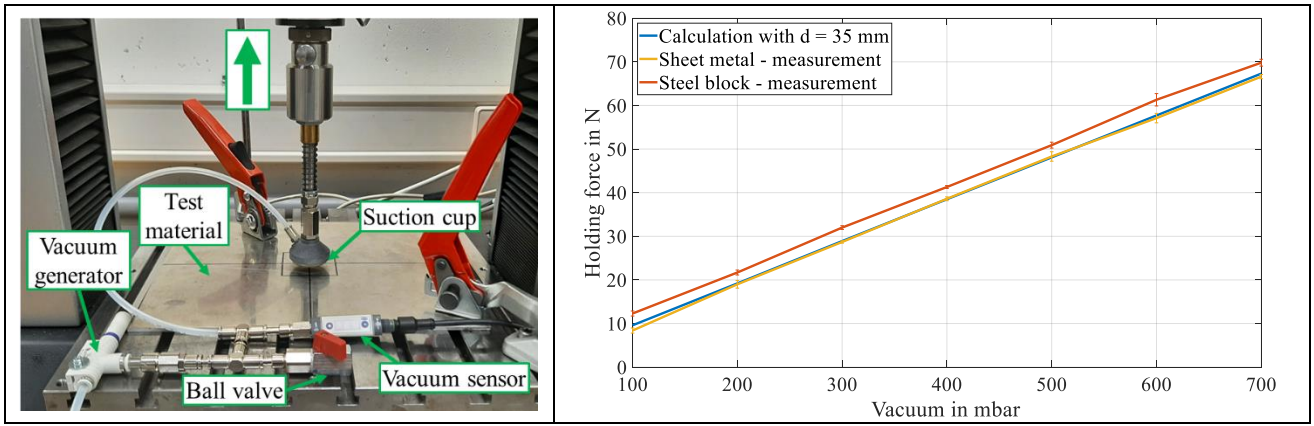


**Figure 11:** Experimental setup and results of the tear-off test

The test results show a good match between the calculated and measured values for the normal force to be applied. The effective diameter of the gasket on the sheet metal is very close to the nominal diameter. However, there is a slight deviation in the steel block test.

#### 4.2. Determination of friction coefficients

In a second test, the friction value between the two test objects and the sealing ring was measured at different vacuum levels to compare the tests with the calculation. To do this, the sealing ring was placed in a holder and pressed against the test piece with a defined vacuum. The required vacuum was created using an ejector and adjusted to the desired level using a vacuum sensor and ball valve. The suction cup was then pulled upwards using a tensile testing machine. The force application point of the tensile machine on the suction cup is as close as possible to the surface of the test piece so that the lowest possible torque occurs during removal. The highest force value is then used to evaluate the force-displacement characteristic. This corresponds to static friction. Once the static friction limit has been exceeded, the suction cup will slip, which would correspond to a failure of the system in a real application. The pull-off test was performed at least three times for each vacuum level tested. Based on the results of section 4.1, the applied normal force  $F_{Nf}$  can be determined and then, using the static friction force  $F_{Sf}$  recorded in the test, the corresponding static friction coefficient  $\mu$  can be determined as follows [12]:

$$\mu = F_{Sf}/F_{Nf} \quad (29)$$

The test setup described and the results of the test with a 35 mm sealing ring are shown in **Figure 12**.

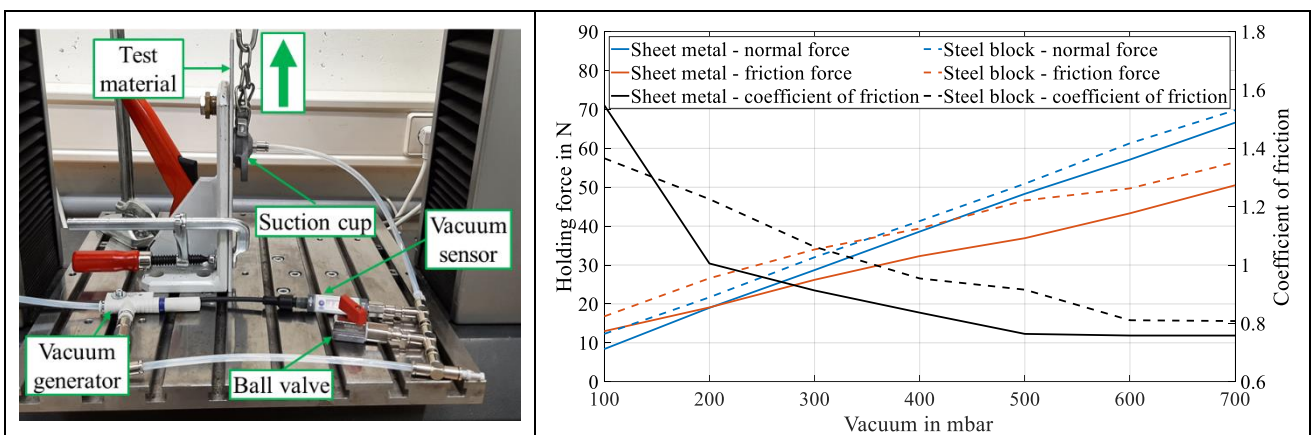


**Figure 12:** Experimental setup and results of the friction test

The results in **Figure 12** show that the coefficient of friction  $\mu$  decreases as the normal force  $F_{Nf}$  increases.

### 4.3. Determination of the holding force as a function of the angle

The following test is carried out to validate the calculation approaches from section 3.1 and 3.2. A frame is used to set and fix the suction cup at a specific angle. The test piece is then sucked in the centre. The necessary vacuum is created by an ejector. A proportional valve then automatically releases air into the system so that the vacuum level in the system is continuously reduced. To slow down and stabilise the venting process, a tank is installed between the ejector and the valve. This also smooths any pressure fluctuations in the system. For the test, the vacuum in the system is reduced until the test part detaches from the suction cup and falls off. The vacuum curve is continuously recorded by three vacuum sensors mounted directly behind the sealing ring using a programmable logical controller (plc) with a cycle time of 1 ms. The arithmetically averaged vacuum curve can be used to determine the vacuum value at which the test piece releases from the suction cup. Using the vacuum value and the seal diameter, equation (1) can be used to determine the theoretical holding force  $F_{Th}$  required during disengagement. The holding force determined in this way is the same as the theoretical holding force determined by the methods described in sections 3.1 and 3.2. The test is carried out for 3 different sealing ring diameters. In order to record a complete curve, the test is repeated in  $10^\circ$  steps and at least five times per step. The test is also carried out for both test objects. The corresponding test setups are shown in **Figure 13**.

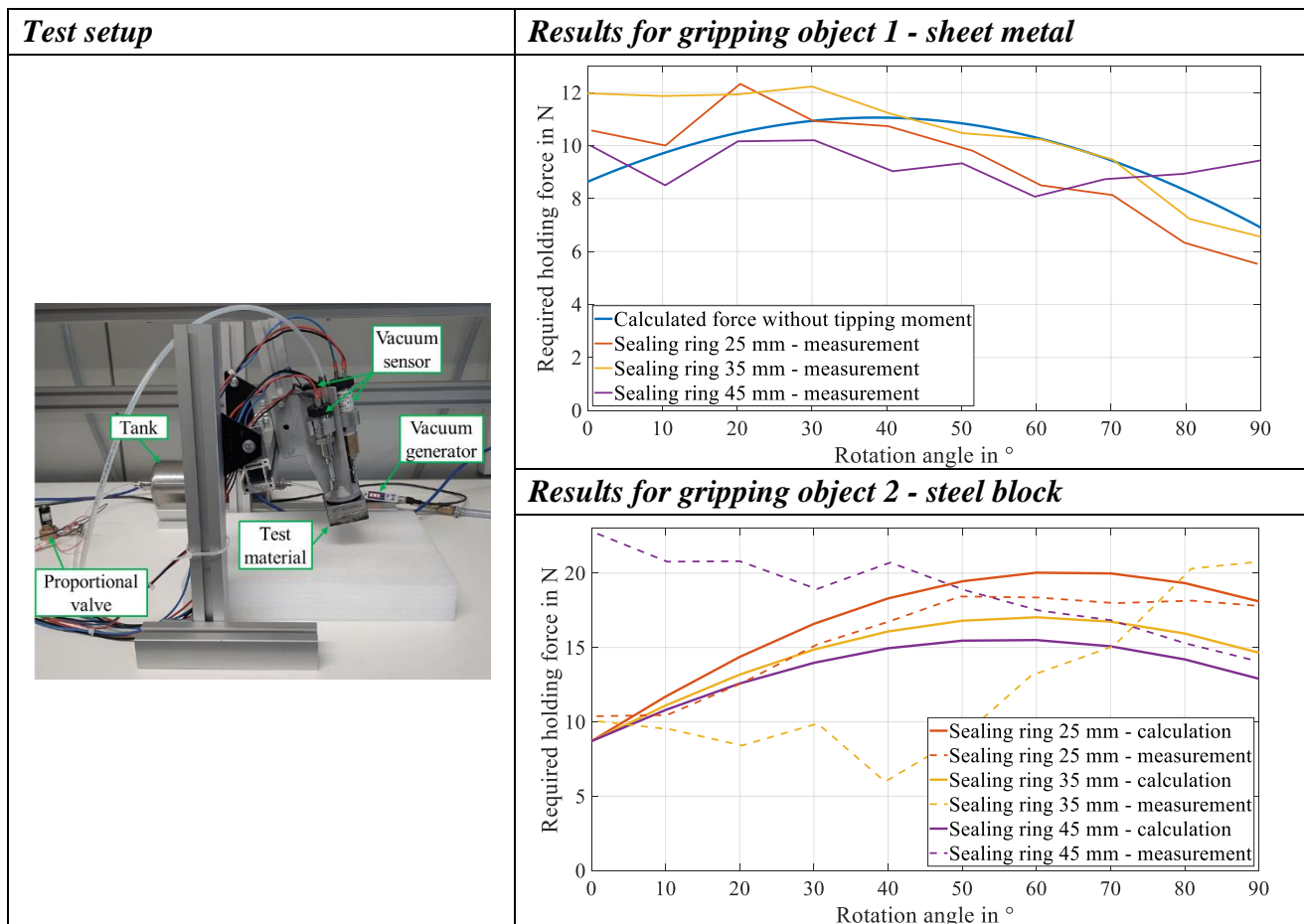


**Figure 13:** Test set-up and results of the holding force test

The process of gripping failure and thus the falling of objects due to the venting of the system is a highly dynamic process. Thus, it is difficult to determine the exact point of detachment. Several types of sensors (triangulation, hall and acceleration sensors) were tested to determine the detachment point. However, these were much slower than the vacuum sensors and only detected a detachment when the

vacuum sensors had already detected ambient pressure again. Therefore, for the evaluation, the detachment point was placed at the beginning of the abrupt pressure change.

As can be seen in **Figure 14**, the deviation of the release points over the series of measurements was significantly smaller for the small seal. However, the deviations for the larger seals were significantly higher.

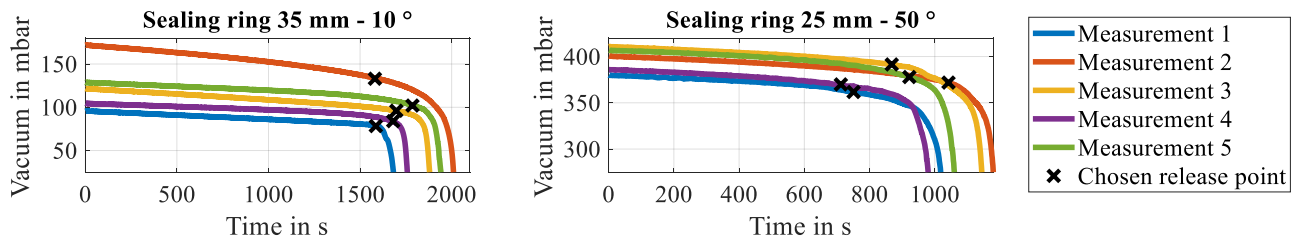


**Figure 14:** Pressure curve and the chosen release point

In addition, a constant static friction value from **Figure 12** was assumed for the calculation, which is approximately at the pressure level of the separation process.

The comparison of the test results with the calculated values shows that there is a good overlap for all sealing ring diameters for the "sheet metal" gripping object. The comparison for the second gripping object "steel block" shows that for the small seal diameter there is a very good match between calculation and test. For the larger ring diameters there are larger deviations in the range between 20 and 70°. However, the exact cause could not be determined with certainty due to the large number of possible influences. However, with the larger ring diameters the pressure in the system increases more slowly prior to separation than with the smaller ring diameters, making it more difficult to determine a specific detachment point.

## 5. CONCLUSION AND OUTLOOK

This paper addresses the challenge of efficient and safe design of vacuum handling systems. A review of the state of the art shows that, apart from a few discrete positions of the gripping object and the surface gripper, no other intermediate positions are considered when calculating the theoretically required holding force for handling gripping objects with surface grippers. Furthermore, the tipping moment due to spatial expansion of the gripping object is neglected. These aspects are taken into account in two new calculation approaches. The first approach extends the current state of the art to include additional intermediate positions for the gripping object and the gripper. The load cases known from the state of the art represent discrete individual positions. The second approach extends the first approach and takes the spatial expansion of the gripping object into account too. To validate the two calculation approaches, different static gripper gripping object positions were experimentally investigated. It was found that the experimental results for a small sealing ring were in very good agreement with the calculated values. Larger deviations occurred only for larger ring diameters and when the tipping moment was taken into account. The cause of these deviations could not be clearly identified due to the large number of influencing factors. Future work will focus on further detailing the calculation approach and extending it to the application of spatial and eccentric forces. It would also be interesting to quantify the reduction in energy consumption in various industrial application scenarios. In addition, most gripper systems use more than one suction cup. This therefore represents another research gap for future work.

## 6. ACKNOWLEDGEMENTS

This work was supported by the Landesministerium für Wissenschaft, Forschung und Kunst Baden Württemberg (Ministry of Science, Research and the Arts of the State of Baden-Württemberg) within

the Nachhaltigkeitsförderung (sustainability support) of the projects of the Exzellenzinitiative.

## NOMENCLATURE

$a$	Acceleration	m/s <sup>2</sup>	$M_S$	Restoring force torque	Nm
$b$	Gripping object support width	m	$M_{Th}$	Theoretical holding force torque	Nm
$d$	Diameter	m	$m$	Gripping object weight	kg
$F_A$	Inertia force	N	$n_3$	Deformation coefficient	-
$F_G$	Weight force	N	$\Delta p$	Differential pressure	Pa
$F_R$	Frictional force	N	$p_0$	System pressure	Pa
$F_S$	Restoring force	N	$p_U$	Ambient pressure	Pa
$F_{Suction}$	Applicable suction force	N	$S$	Safety factor	-
$F_{Th}$	Theoretical holding force	N	$t$	Time	s
$g$	Acceleration due to gravity	m/s <sup>2</sup>	$\alpha$	Rotation angle	°
$h$	Gripping object height	m	$\eta$	Efficiency due to leakage losses	-
$M_A$	Inertia force torque	Nm	$\mu$	Coefficient of static friction	-
$M_G$	Weight force torque	Nm			

## REFERENCES

- Gabriel F, Bobka P, Dröder K (2020) Model-Based Design of Energy-Efficient Vacuum-Based Handling Processes. *Procedia CIRP* 93:538–543. <https://doi.org/10.1016/j.procir.2020.03.006>
- Straub D (2020) Methode zur technischen Auslegung von Vakuumgreifsystemen mit einer Mindesthaltedauer auf Basis fluidischer Untersuchungen. Dissertation
- Stegmaier V, Schaaf W, Jazdi N et al. (2023) Simulation Model for Digital Twins of Pneumatic Vacuum Ejectors. *Chem Eng & Technol* 46:71–79. <https://doi.org/10.1002/ceat.202200358>
- Straub D, Huber K (2018) Potentials of vacuum gripping systems in human-robot-collaboration applications. VDE Verlag, Berlin, Offenbach
- Fritz F, von Grabe C, Kuolt H et al. Benchmark of existing energy conversion efficiency definitions for pneumatic vacuum generators. [https://doi.org/10.1007/978-981-4451-48-2\\_22](https://doi.org/10.1007/978-981-4451-48-2_22)
- Stegmaier V, Schaaf W, Jazdi N et al. (2022) Anwendungsfälle und Ansatz zur Erstellung des Digitalen Zwillings aus Sicht eines Komponentenherstellers. In: *Automation 2022*: 23. Leitkongress der Mess- und Automatisierungstechnik : automation creates sustainability : Baden-Baden, 28. und 29. Juni 2022. VDI Verlag, Düsseldorf, pp 5–18
- Stegmaier V, Eberhardt T, Schaaf W et al. (2023) Automated Configuration of Optimized Customer Specific Mechatronic Systems Using Behavior Models. *CIRP Conference on Intelligent Computation in Manufacturing Engineering*. <https://doi.org/10.13140/RG.2.2.21121.22889>
- Hesse S (1997) Greiferanwendung: Blue Digest on Automation
- Festo Didactic GmbH & Co. KG Grundlagen der Vakuumtechnik: Kurzübersicht. [https://www.festo.com/net/supportportal/files/9916/grundlagen\\_vakuumtechnik.pdf](https://www.festo.com/net/supportportal/files/9916/grundlagen_vakuumtechnik.pdf). Accessed 10 Oct 2023
- J. Schmalz GmbH Theoretische Haltekraft eines Sauggreifers: Typische Lastfälle. <https://www.schmalz.com/de-de/vakuum-wissen/vakuumsystem-und-seine-bauteile/systemauslegung-berechnungsbeispiel/theoretische-haltekraft-eines-sauggreifers/>. Accessed 10 Oct 2023
- Spivak D (2021) The Science of Vacuum-Cup Forces. <https://fluidpowerjournal.com/the-science-of-vacuum-cup-forces/>. Accessed 10 Oct 2023
- Kern P Elastomerreibung und Kraftübertragung beim Abscheren von aktiv betriebenen Vakuumgreifern auf rauen Oberflächen. Dissertation, Karlsruher Institut für Technologie (KIT); Karlsruher Institut für Technologie